Electromagnetic Coupling on an Atomic Scale

J. Aizpurua,[1] G. Hoffmann,[2,*] S. P. Apell,[3] and R. Berndt[2]

[1]*National Institute of Standards and Technology, Gaithersburg, Maryland 20899-8423*
[2]*Institut für Experimentelle und Angewandte Physik, Christian-Albrechts-Universität zu Kiel, D-24098 Kiel, Germany*
[3]*University Outreach, Kristianstad University, SE-291 88 Kristianstad, Sweden*

(Received 17 May 2002; published 24 September 2002)

Light emission from a scanning tunneling microscope is used to investigate the electromagnetic coupling (EMC) of a metal tip and a metal sample. Subatomic scale modifications of the tip-sample region cause spectral shifts of the fluorescence as demonstrated for a monatomic step and by variation of the tip-sample distance. For sharp tips the EMC is confined to a lateral range of a few nm. The results are consistent with model calculations of the electromagnetic response of an appropriate tip-sample geometry.

DOI: 10.1103/PhysRevLett.89.156803 PACS numbers: 73.20.Mf, 68.37.Ef, 73.21.–b, 78.67.–n

The electromagnetic interaction between objects in nanometer proximity plays a central role in surface enhanced Raman scattering. Moreover, it is vital to scanning probe techniques such as noncontact atomic force microscopy (AFM) [1] or scanning near-field optical microscopy [2]. The electromagnetic coupling of the tip and the sample leads to the formation of new, localized electromagnetic modes. In a scanning tunneling microscope (STM), these modes can be excited by inelastic electron tunneling and give rise to the emission of characteristic fluorescence [3–8]. Spectral analysis of this fluorescence can be used to study the electromagnetic coupling on an atomic scale. Here we address the interaction of these modes with a simple model structure, namely, an atomic step. More specifically, we report the gradual changes that occur in fluorescence spectra while the STM tip passes a monatomic step in a lateral direction. From the spectral shifts as a function of the distance to the step the lateral extension of the surface plasmon mode induced at the cavity is estimated. The data are analyzed quantitatively using model calculations where the tip is assumed to be a revolution hyperboloid with a radius of curvature of a few nm. We note that results for simple structures such as steps may also be useful in understanding more complex situations where the electromagnetic coupling (EMC) at the cavity is also altered by the presence of an atomic scale modification such as an adsorbed molecule. Indeed, the fluorescence spectra recorded from some particular molecules can hardly be distinguished from those of the metal substrate except for a small overall shift of the spectrum [9]. The shifts observed here also bear similarity to electrostatic interaction forces in AFM of monatomic steps [10]. Understanding the implications of subatomic modifications of the cavity and its spatial extension is therefore relevant for a variety of situations.

Fluorescence measurements were performed with a STM in ultrahigh vacuum (UHV) at low temperature (5 K) equipped with a lens system along with a CCD camera and a grating spectrometer [11]. Au and Ag (111) surfaces as well as Au and Ag-covered W tips were prepared in UHV by standard Ar ion sputtering and annealing cycles. The status of the surface was verified before and after all experiments with STM to rule out modifications during the measurement.

Figure 1 shows experimental data recorded from a monatomic step on Ag(111). This step was straight over a distance of ≈ 300 Å. The solid line represents a cross-sectional profile of a constant current topograph. At each STM image point a fluorescence spectrum was recorded.

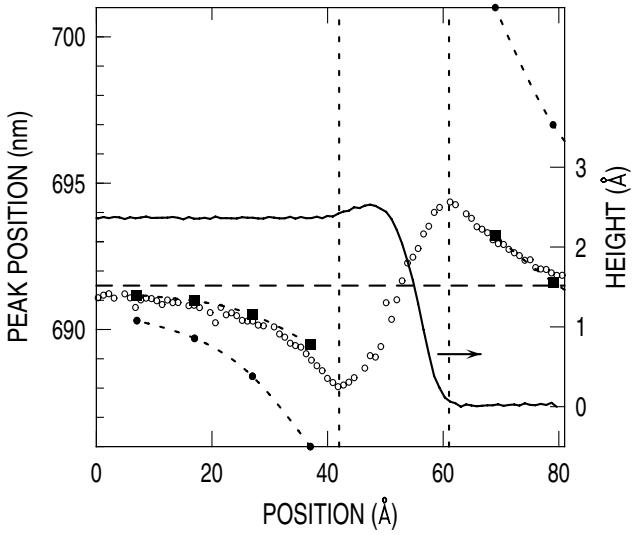

FIG. 1. Cross-sectional profile of a constant current topograph from a monatomic step on Ag(111) (line) at a sample voltage $V = 2.9$ V and a tunneling current $I = 5$ nA, along with peak positions (circles) from fluorescence spectra recorded at each STM image point. Model calculations for an axially symmetric step are indicated by dots ($\Delta\lambda_{\text{island}}$). Corrected values for a one-dimensional step are plotted as squares ($\Delta\lambda_{\text{step}}$). Vertical dashed lines delimit the immediate proximity of the step where significant vertical tip motion occurs.

From the spectra overall shifts of the emission are observed while the spectral shape remains unaffected. To quantify these shifts, Fig. 1 (circles) displays the wavelengths of the peak versus the tip position. As the tip approaches the step from the upper atomic terrace, the emission shifts to shorter wavelength, whereas a redshift occurs when approaching from the lower terrace. The shifts are detected up to a lateral distance of ≈ 50 Å from the step, which is consistent with model calculations for the extension of the mode at the cavity [12].

To interpret this spectral shift we connect the lateral extension of the surface mode induced at the cavity with the vertical tip-sample distance d. If we consider the modes of a vacuum gap of width d between a semi-infinite free-electron metal sample and a sharp tip, the lowest energy mode disperses with d according to $\hbar\omega \sim d^{1/n}$, where n depends on the geometry of the tip [13]. This mode, which corresponds to charges of opposite signs on the boundaries, causes the light emission in STM [4]. For increasing tip-sample distance d a blueshift occurs as observed on the upper terrace when the tip is approaching the step. Apparently, the presence of the down step causes an effective increase of d shifting the fluorescence peak position accordingly. Since the shift in the emission peak appears as a consequence of the interaction of the surface mode with the step, we estimate the extension of the mode as the distance where the shift becomes noticeable, in our case ≈ 50 Å.

To test experimentally the spectral shift as a function of tip-sample distance d, we also varied d over a perfectly flat surface sample, i.e., in absence of steps, and simultaneously recorded fluorescence spectra. However, as d increases, the tunneling current I, which serves to excite the photon emission, decreases exponentially. In addition, d should not be too small since large currents eventually cause sample damage. Thus, low-photon count rates previously prevented spectrally resolved measurements. Using an efficient detection scheme, this limitation can to some extent be overcome, and statistically significant fluorescence spectra can be acquired over a range of distances.

For reference, Fig. 2 shows a fluorescence spectrum obtained at a sample voltage $V = 3$ V on an extended, defect-free terrace of a Au(111) surface. An intensity peak occurs at a wavelength $\lambda \approx 660$ nm with broad tails to both sides, which corresponds to the plasmon resonance for the given d and tip shape. V was chosen sufficiently large to have the peak fully developed. The spectrum is similar to previously reported and calculated spectra from Au tips on Au samples [14,15].

Starting from the conditions used in Fig. 2, some 680 fluorescence spectra were recorded at increasing tip-sample distances. In addition to an expected exponential variation of the intensity, we observe an overall blueshift of the emission while the spectral shape remains unaffected. Figure 3 displays the mean emission wavelength $\overline{\lambda}$ versus the tunneling current and the associated

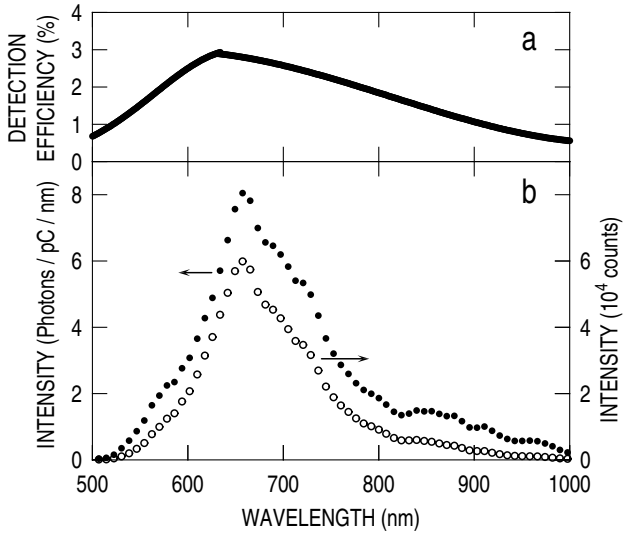

FIG. 2. (a) Wavelength dependent detection efficiency of the optical setup. (b) Fluorescence spectrum of a flat Au(111) surface and a Au tip at a sample voltage $V = 3$ V and a tunneling current $I = 34$ nA as measured (circles) and corrected for the detection efficiency (dots).

tip excursion. Here $\overline{\lambda}$ is defined as $\overline{\lambda} = \int \lambda P(\lambda)\, d\lambda / (\int P(\lambda)\, d\lambda)$, where P is the spectral density of the fluorescence. Using this definition, smaller shifts can be resolved [16]. The peak position is offset from $\overline{\lambda}$ by (-20 ± 4) nm. The uncertainty of the peak position is the root mean square or combined standard uncertainty of the statistical uncertainty (less than ± 1 nm), and the systematic uncertainty (± 4 nm). We observe an approximately linear blue-shift of $\overline{\lambda}$ with the tip excursion Δd, at a slope of 3 nm/Å [17].

For a quantitative analysis, we model the tip as a hyperboloid with aperture angle ϕ and tip apex parameter b

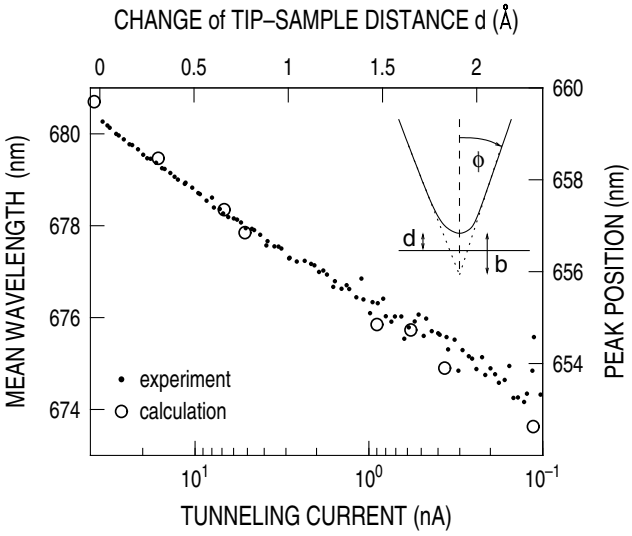

FIG. 3. Mean wavelength of emission $\overline{\lambda}$ (and emission peak position) vs tunneling current and associated vertical tip displacement, as measured (dots) and calculated (circles). The inset shows the tip shape used for modeling the data.

located at a distance d above the flat surface (see inset of Fig. 3) [12]. The radius of curvature of the tip is $R = b\tan(\phi)$. In our model the emission peak is an incoherent sum of the inelastic transitions of energy $\hbar\omega$ between tip and sample states at energies E_t and E_s associated with the current density $\vec{j}_{ts}(\vec{r}', \omega)$ weighted by the field enhancement at the cavity $G(\vec{r}', \omega)$. The radiated power per photon energy and solid angle is

$$\frac{d^2P}{d\Omega d(\hbar\omega)} = \frac{\omega^2}{8\pi^2\varepsilon_o c^3}\sum_{t,s}\left|\int d^3\vec{r}'\, G(\vec{r}', \omega)\,\vec{j}_{ts}(\vec{r}', \omega)\right|^2 \times \delta(E_t - E_s - \hbar\omega), \quad (1)$$

where c is the velocity of light. The field enhancement factor $G(\vec{r}', \omega)$ determines the modes at the cavity which can decay into photons, and is calculated numerically with a boundary element method using bulk dielectric functions [18]. This approximation is acceptable [19]. The tunneling current is obtained from the model of Tersoff and Hamann extended to high energy losses [12,20]. On the surfaces considered here most of the spectral structure is due to G, while—at eV sufficiently larger than the energy of the plasmon resonance—the spectrum of $\vec{j}_{ts}$ causes only small modifications.

All geometrical parameters describing the tip (ϕ, b, and d) influence the peak position, but the overall aperture of the tip ϕ is responsible for the rough position of the emission peak. Small changes of this parameter can lead to wavelength changes of several 10 nm. On the other hand, the tip-sample distance d and the apex length parameter b control a fine tuning of the peak position. b also affects the shift of the peak with vertical tip excursion from ≈ 3 nm/Å for sharp tips ($R = 10$ Å) up to ≈ 10 nm/Å for blunt tips ($R > 150$ Å). Once ϕ and b are chosen to be consistent with the experimental spectra, d is varied as in the experiment. The resulting calculated peak positions are shown in Fig. 3 (circles). We obtain a quantitative agreement with the experiment for an open tip ($\phi = 40°$) with a sharp apex ($R = 10$ Å) which is a typical value for atomic resolution tips [21].

Having determined the effect of the tip-sample distance d on the fluorescence spectra of a perfectly flat surface, we are now in a position to further analyze the data of Fig. 1 near the step. To model tip positions outside the immediate proximity of the step [22], the straight step of the experiment is replaced by a cylindrical hole (or island) of height $h_0 = 2.36$ Å [Ag(111) interlayer spacing] as shown in Fig. 4(a) (top). While this geometry clearly overestimates the influence of a step, its symmetry keeps the numerical expense acceptable. The radius ρ of the hole (or island) is set to the experimental, lateral distance from the step. As in the experiment, the calculated spectral shape does not change as ρ is varied while there are clear overall shifts. The shifts evaluated from the spectra are indicated by dots in Fig. 1. In agreement with experiments we find a blueshift when the tip is located on the top of a progressively narrower island and a redshift when it is located on the bottom of a progressively narrower hole. Figure 4(b) shows the calculated sample charge densities of the mode responsible for light emission in the present experiment together with the sample topography for three distances to the step ($\rho =$ 15, 35, and 55 Å). We define the EMC to be the spatial extent of the induced surface plasmon. For a tip with radius $R = 10$ Å, the EMC extends over a lateral range of only ≈ 20 Å as determined by the full width at half maximum of the plasmon charge density, although the tail of the plasmon extends up to more than twice this value, as shown in Fig. 4(b). The localized mode at the sample surface suffers a stronger modification as the center of the mode (tip position) is closer to the monatomic step. When the lateral distance to the step is of the order of the mode extension or larger, the surface charge

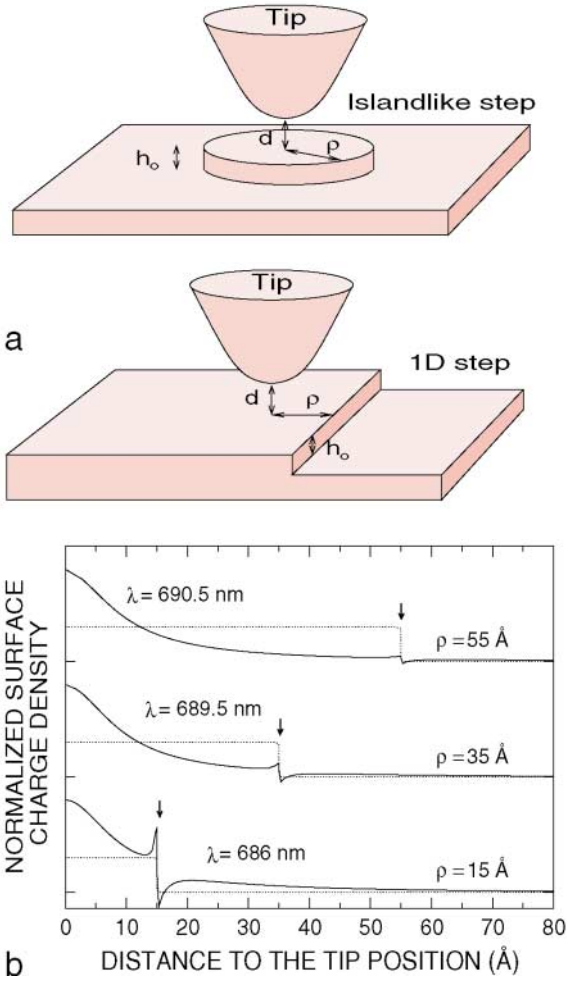

FIG. 4 (color online). (a) Geometries used to model light emission near a step. Top: Step showing azimuthal symmetry to obtain Δ_{island} in Fig. 1. Bottom: One dimensional step used for obtaining the corrected Δ_{step} in Fig. 1. (b) Cross section of the calculated surface charge densities (solid lines) at the sample for three lateral distances ($\rho = 15$, 35, and 55 Å) of the tip to the step marked with arrows. Topography is indicated by a dotted line. The surface charge density is more strongly modified as the tip is located closer to the step ($\rho = 15$ Å).

density is not affected any more and the emission of a perfectly flat surface is recovered. From the calculations in Fig. 4, it is noticeable that this limit is already being reached at a lateral distance of $\rho = 55$ Å. The lateral distance where the shift becomes discernible is therefore connected with the range of the interaction of the plasmon mode with the step. Both the model calculations presented in Fig. 4(b) and the experimental extension agree at a value of ≈ 50 Å.

As expected, the calculated shifts for this model are larger than the experimental data. This discrepancy can be corrected as follows. We demonstrated that a change Δd of the tip-sample distance leads to a linear shift of the spectral maximum: $\Delta\lambda \sim \Delta d$. From the calculation we find a lateral extension of the plasmon on a nanometer scale ($\approx$50 Å). Any variation of the surface height $h(\vec{r})$ within this range will effectively change the average tip-sample distance. Therefore, we define an effective distance d_{eff} given by $d_{\text{eff}} = d + \Delta d_{\text{eff}}$ where

$$\Delta d_{\text{eff}} = \int \sigma_s(\vec{r}) h(\vec{r}) d^2\vec{r}. \tag{2}$$

σ_s is the normalized [$\int \sigma_s(\vec{r}) d^2\vec{r} = 1$] charge density of the plasmon mode on the sample surface as calculated. This convolution of height change and surface charge density accounts for any surface variation over the area where the surface plasmon extends. For a hole (or island), $h = 0$ within a circle of radius ρ, and $h = \pm h_0$ outside (see top of Fig. 4). Similarly, for the case of a one-dimensional ascending or descending step at $x = \rho$, we have $h = \pm h_0$ for $x > \rho$ and $h = 0$ elsewhere (bottom of Fig. 4). The shift $\Delta\lambda_{\text{island}}$ originally calculated for the case of an axially symmetric step is then corrected by the right convolution with the more realistic geometry:

$$\Delta\lambda_{\text{step}} = \frac{\Delta d_{\text{step}}}{\Delta d_{\text{island}}} \Delta\lambda_{\text{island}}. \tag{3}$$

The resulting data shown as squares in Fig. 1 are close to the measured spectral shifts. We note that the presence of a second descending step at the position 125 Å is also taken into account in calculating $\Delta\lambda_{\text{step}}$.

In summary, we have demonstrated experimentally that the electromagnetic coupling of a metal tip and a metal sample varies upon sub-Å variations of their distance, leading to measurable spectral shifts of the lowest localized plasmon resonance. This effect explains spectral shifts occurring near atomic steps on the sample surface and allows a direct measurement of the lateral extension of the localized surface plasmon on the surface. For sharp tips we find lateral extensions of the coupling in the range of a few nanometers, consistent with model calculations of the electromagnetic response of a tip-sample geometry.

We are delighted to thank A. Baratoff for discussions. This work has been supported by the European Commission via the TMR network EMIT and by the Deutsche Forschungsgemeinschaft.

*Present address: Institut of Applied Physics, University of Hamburg, Germany.

[1] See, e.g., *Forces in Scanning Probe Methods*, edited by H.-J. Güntherodt, D. Anselmetti, and E. Meyer, NATO ASI, Ser. E, Vol. 286 (Kluwer, Dordrecht, 1995).
[2] *Near Field Optics*, edited by D.W. Pohl and D. Courjon, NATO ASI, Ser. E, Vol. 241 (Kluwer, Dordrecht, 1993).
[3] J. K. Gimzewski, J. K. Sass, R. R. Schlittler, and J. Schott, Europhys. Lett. **8**, 435 (1989).
[4] P. Johansson, R. Monreal, and P. Apell, Phys. Rev. B **42**, 9210 (1990).
[5] R. Berndt, J. K. Gimzewski, and P. Johansson, Phys. Rev. Lett. **67**, 3796 (1991).
[6] B. N. J. Persson and A. Baratoff, Phys. Rev. Lett. **68**, 3224 (1992).
[7] M. Tsukada, T. Schimizu, and K. Kobayashi, Ultramicroscopy **42-44**, 360 (1992).
[8] S. Ushioda, Y. Uehara, and M. Kuwahara, Appl. Surf. Sci. **60/61**, 448 (1992).
[9] G. Hoffmann, L. Libioulle, and R. Berndt, Phys. Rev. B **65**, 212107 (2002).
[10] M. Guggisberg *et al.*, Surf. Sci. **461**, 255 (2000).
[11] G. Hoffmann, J. Kröger, and R. Berndt, Rev. Sci. Instrum. **73**, 305 (2002).
[12] J. Aizpurua, S. P. Apell, and R. Berndt, Phys. Rev. B **62**, 2065 (2000).
[13] R.W. Rendell, D. J. Scalapino, and B. Mühlschlegel, Phys. Rev. Lett. **41**, 1746 (1978).
[14] R. Berndt, J. K. Gimzewski, and P. Johansson, Phys. Rev. Lett. **71**, 3493 (1993).
[15] R. Péchou *et al.*, J. Phys. III (France) **6**, 1441 (1996).
[16] This procedure is acceptable since the spectral shape does not change significantly over the range of distances probed here.
[17] In Ref. [14], due to limited efficiency of the photon detection, isochromat emission intensities were analyzed rather than fluorescence spectra. The present results shed new light on these earlier data. Since the entire emission spectrum is found to redshift as the tip-sample distance decreases, one may obtain an increase or decrease of the isochromat intensity depending on the wavelength considered.
[18] *Handbook of Optical Dielectric Constants of Solids*, edited by D. Palik (Naval Research Laboratory, Washington DC, 1985).
[19] P. Johansson, Phys. Rev. B **58**, 10 823 (1998).
[20] K. Stokbro, U. Quaade, and F. Grey, Appl. Phys. A **66**, S907 (1998).
[21] J. Tersoff and D. R. Hamann, Phys. Rev. B **31**, 805 (1985).
[22] On the terraces $\vec{j}_{ts}(r)$ is constant. At tip positions in close proximity to the step (indicated by dashed vertical lines) significant vertical excursion of the tip occurs which may affect the spectrum of $\vec{j}_{ts}$. Quantitative modeling of this area requires knowledge of the atomic tip structure.